

Fabrication and characterization of hydroxyapatite-coated forsterite scaffold for tissue regeneration applications

ROYA SAIDI^{1,*}, MOHAMMAD HOSSEIN FATHI^{1,2} and HAMIDREZA SALIMIJAZI³

¹Biomaterials Research Group, Department of Materials Engineering, Isfahan University of Technology, Isfahan 8415683111, Iran

²Dental Materials Research Center, Isfahan University of Medical Sciences, Isfahan 8174673461, Iran

³Department of Materials Engineering, Isfahan University of Technology, Isfahan 8415683111, Iran

MS received 19 April 2015; accepted 8 May 2015

Abstract. In this study, a novel hydroxyapatite (HA)-coated forsterite scaffold with a desired porous structure, high mechanical properties and good bioactivity was successfully fabricated via gel-casting and sol-gel in low pressure methods. X-ray diffraction, scanning electron microscopy, transmission electron microscopy and X-ray map techniques were utilized in order to evaluate the phase composition, dimension, morphology, interconnectivity of the pores and state of the coating on the porosities of the synthesized scaffold. The porosity and compressive strength of the scaffolds were measured and the bioactivity was investigated by soaking the scaffolds in simulated body fluid (SBF). The results show that the prepared scaffolds had highly interconnected spherical pores with size in the range of 65–245 μm . Additionally, compressive strength and elastic modulus were 7.5 ± 0.2 and 291 ± 10 MPa, respectively. The crystallite size of the scaffolds was less than 60 nm. True (total) and apparent (interconnected) porosity of the scaffolds were in the range of 75–80 and 65–70%, respectively. *In vitro* tests in the SBF also confirmed good bioactivity of the prepared scaffolds. While bone-like apatite formation started from the first day of soaking and apatite covered the entire surface and inner wall of the scaffolds pores at long immersion time. Conclusion suggested that HA coating on forsterite scaffolds could significantly improve the mechanical properties and bioactivity, which might be promising for tissue engineering applications.

Keywords. Ceramics; mechanical alloying; gelcasting process; porosity; mechanical properties.

1. Introduction

Bioactive materials with different properties are used for bone repair and bone tissue engineering applications.¹ Easy production and good biocompatibility of bioceramics make them the most important group of biomaterials.^{2,3} Nowadays much attention is paid to porous bioceramics, foams or scaffolds.⁴ An ideal scaffold intends to mimic the mechanical and biochemical properties of the native tissue.⁵

Hydroxyapatite (HA) is the most widely used bioscaffolds in hard tissue repair due to its chemical and crystallographic resemblance to the mineral component of human bone and teeth. It also has excellent biocompatibility, bioactivity, osteoconduction and osteointegration properties.^{6–9} However, its brittleness and weak mechanical properties such as low fracture toughness restrict its use in load-bearing applications.^{3,8,10,11} To be used effectively in such applications, the mechanical properties of

HA need to be improved.¹² The incorporation of other ceramics with better mechanical properties such as forsterite (Mg_2SiO_4) might improve the mechanical properties of HA.¹³

Forsterite is a crystalline magnesium silicate, which belongs to the group of olivine.^{8,14–16} In recent years, forsterite has gained popularity due to its wide range of applications. This bioceramic is a biocompatible material with high mechanical properties.^{2,4,10,16–19} Comparison to calcium phosphate ceramics such as HA ($\text{KIC} = 0.75\text{--}1.2 \text{ MPa m}^{1/2}$), forsterite ceramics showed a significant improvement in the fracture toughness ($\text{KIC} = 2.4 \text{ MPa m}^{1/2}$) and were superior to the lower limit reported for cortical bone. This makes forsterite as a possible candidate for load-bearing applications.^{3,20–22}

Ghomi *et al.*⁴ fabricated forsterite scaffold via the gel-casting method. The scaffold had compressive strength of about 2.5 MPa, which is not good enough for load-bearing applications.

The aim of this work was to develop a new route to enhance the compressive strength of forsterite scaffold via two-step sintering process of forsterite scaffolds and coating with HA.

*Author for correspondence (r.saidighahe@ma.iut.ac.ir)

2. Experimental

2.1 Synthesis of nanostructured forsterite powder

A mixture of magnesium hydroxide carbonate ($4\text{MgCO}_3 \cdot \text{Mg}(\text{OH})_2 \cdot 5\text{H}_2\text{O}$, Merck) and silicon dioxide (SiO_2 , Merck) was mechanically activated using a high-energy planetary ball mill for 10 h under ambient condition. Zirconia vial and five zirconia balls with a diameter of 20 mm were utilized as milling media. Mechanical activation was performed using ball/powder mass ratio of 12.5:1 and rotation speed of 250 rpm. The prepared powder was then heated at 900°C for 1 h in air atmosphere and isothermal condition.

2.2 Fabrication of forsterite scaffold

Forsterite scaffold was prepared by the gel-casting method; an effective process for the fabrication of highly porous ceramics.²³ For this purpose, forsterite powder was added to a solution of 1 wt% tripolyphosphate sodium as a dispersant in deionized water to make a suspension of 45 wt% solid loading. Coincidentally, agarose (a gelling agent) solution in deionized water (7 wt%) was warmed up to 80°C . Later, the agarose solution was added to the forsterite slurry by keeping the temperature of the initial slurry at 80°C to obtain a forsterite suspension. Finally, tergitol as a surfactant was added to the prepared suspension. Foaming was conducted through agitation with the help of a triple-blade mixer at 80°C .⁴ The prepared slurry was poured into the glass molds and cooled to 0°C . The green bodies were then left at room conditions to dry and sintered via two-step sintering process similar to previous reports. The flowchart of two-step sintering process is shown in figure 1.

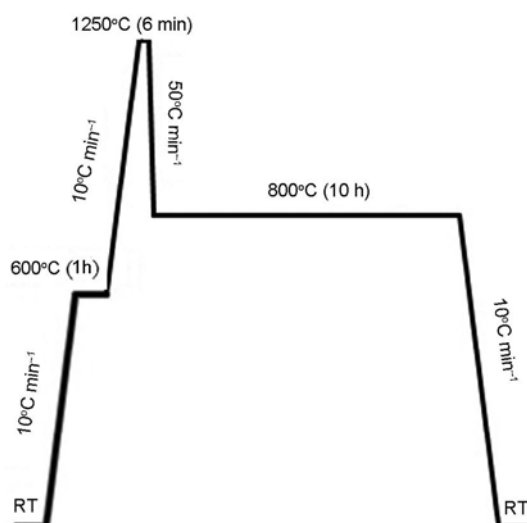


Figure 1. Detailed flowchart of two-step sintering of forsterite scaffold.

2.3 Preparation of HA coating sol

A certain amount of phosphoric pentoxide (P_2O_5 , Merck) was dissolved in perfect ethanol to produce a 0.5 mol l^{-1} solution. At the same time, a designed amount of calcium nitrate tetrahydrate ($\text{Ca}(\text{NO}_3)_2 \cdot 4\text{H}_2\text{O}$, Merck) was also dissolved in absolute ethanol to form a 1.67 mol l^{-1} solution in another beaker. The solutions were mixed with a molar ratio of $\text{Ca/P} = 1.67$ and the initial mixture was prepared.^{24–26} The mixture was continuously stirred for 3 h at ambient temperature to obtain a white transparent gel. After preparing the gel, the forsterite scaffolds were coated via the method mentioned in section 2.3a. After 24 h aging in the ambient temperature, the samples were dried at 80°C for 24 h in an electrical air oven. Finally, the samples were sintered at 600°C for 1 h in a resistance furnace with a heating rate of 5°C min^{-1} .^{24–26}

2.3a Coating forsterite scaffold: As the forsterite scaffold was porous and air is present in the pores, the sol-gel method at low pressure was chosen. This technique provides quick and comfortable coatings of sol, leading to the creation of a uniform coverage. Forsterite scaffold was placed in the beaker inside the desiccator and the inner pressure was set to -0.8 Torr relative to the ambient pressure. When the inner pressure of the desiccator reached the mentioned amount, the hoses connecting the desiccator to the beaker containing the coating sol was opened, and the coating sol entered the beaker inside the desiccator. When the sol encompassed the scaffold, the vacuum was disconnected and the scaffold was excluded.

2.4 Materials characterization

Phase structure characterization of forsterite powder, scaffolds and HA coating were performed using the X-ray diffractometer (XRD) (Philips X'Pert-MPD, $\text{CuK}\alpha$ radiation = 0.154 nm , 2θ range of 20 – 80° , step size: 0.05° and time per step: 1 s).

The crystallite size of forsterite powder and the prepared scaffolds were determined using broadening of XRD pattern peaks and Scherrer's equation²⁷

$$d = \frac{0.89\lambda}{B \cos \theta}, \quad (1)$$

where d is the crystallite size (nm), λ the wavelength ($\lambda = 0.154 \text{ nm}$), B the broadening of diffraction line measured at half its maximum intensity and θ the Bragg angle (deg).

The surface morphology of the scaffolds was studied by field-emission scanning electron microscopy (SEM) (Philips XL30 FEG) coupled with energy-dispersive spectrometer. X-ray map was utilized to evaluate the formation of HA coating on the surface of forsterite scaffold porosities.

Transmission electron microscopy (TEM, Philips GM120FEG) was used to study the morphology and particle size of the prepared scaffold.

The porosity of scaffolds was measured according to the Archimedes principle with distilled water as an immersion medium and by using the theoretical density of 3.221 g cm^{-3} for forsterite.²⁸

In order to determine the mechanical properties of the samples, compressive tests were performed using a compression test machine (Hounsfield, H25KS). For this purpose, the samples were cubed with dimensions $5 \times 10 \times 10 \text{ mm}^3$ and the crosshead speed of 0.5 mm min^{-1} was utilized.^{12,29}

The compressive strength of each scaffold was calculated as the maximum applied force divided by the measured initial bulk cross-sectional area of the specimen, and the elastic modulus was calculated as the slope of the initial linear portion of the stress–strain curve. The final result was presented as the average of three measurements and the standard deviation for HA-coated forsterite scaffold. The bioactivity of the scaffolds was determined *in vitro* through the immersion of prepared samples in SBF as described by Bohner and Lemaître³⁰ at $36.5 \pm 0.5^\circ\text{C}$ for 28 days. As-prepared scaffolds were placed in sterilized bottles with a solid/liquid ratio of 10 mg ml^{-1} . The samples were then filtered, rinsed with distilled water and dried in air. The formation of apatite-like layer on the samples was investigated and studied by SEM. In addition, the SBF solution was also monitored for the changes of pH using an electrolyte-type pH meter (Nethrohm827), and variations in Ca and P ions were evaluated via using inductively coupled plasma optical emission spectrometry (ICP-OES, Perkin Elmer).

3. Results and discussion

Figure 2 shows the XRD patterns of the prepared forsterite powder and forsterite scaffold. It is obvious that only the forsterite peaks existed in the pattern (JCPD

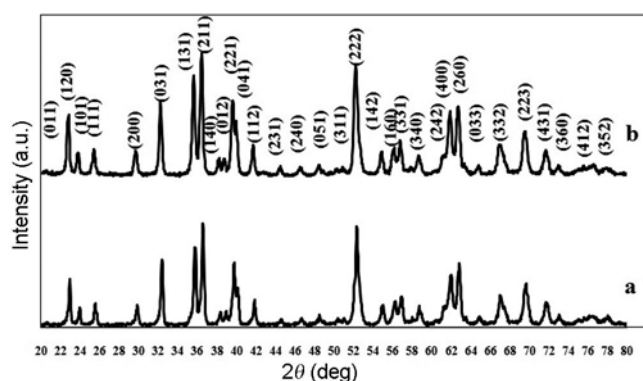


Figure 2. XRD patterns of prepared (a) forsterite nanopowder and (b) forsterite scaffold.

34-0189), indicating successful preparation of a pure forsterite powder and forsterite scaffold. The crystallite size of the forsterite scaffolds was in the range of 35–60 nm by broadening of XRD peaks using Scherrer's formula.

Figure 3 shows TEM micrographs of forsterite scaffold. TEM micrographs show that the particle size is smaller than 150 nm.

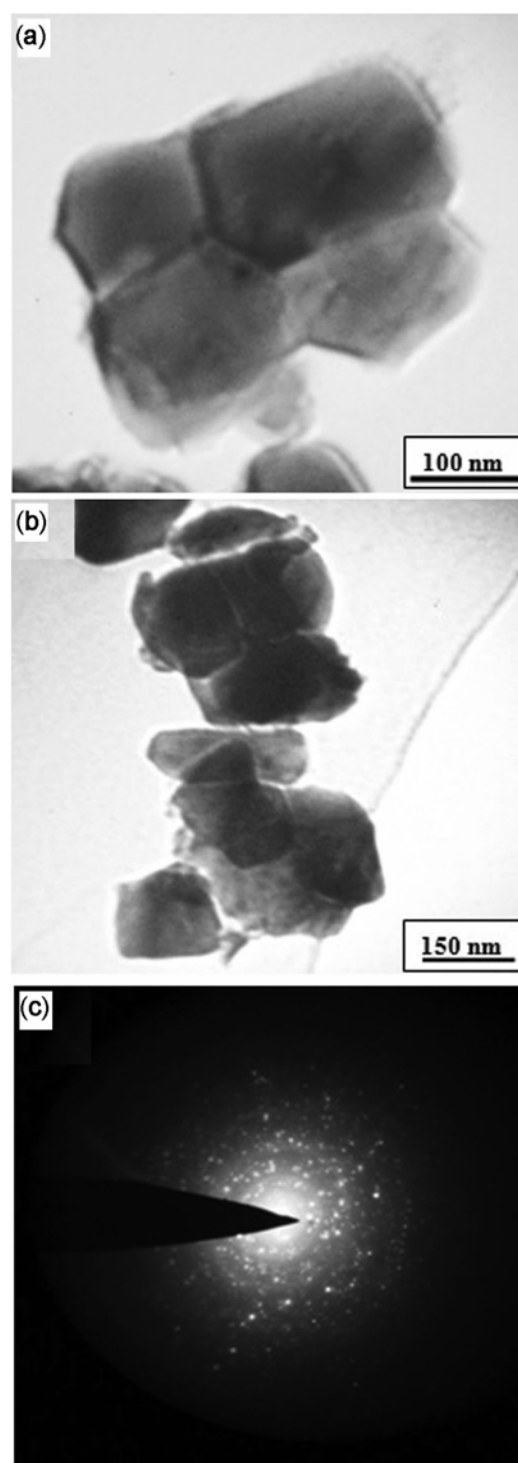


Figure 3. TEM micrographs of the forsterite scaffold.

Figure 4 shows the XRD pattern of the prepared HA coating. The result shows that at 600°C, a HA coating was produced with appropriate phase purity and with the crystallite size in the range of 25–29 nm. All the peaks existing in the pattern belong to HA (JCPD 09-0432),

which is in good agreement with the research carried out by Hanifi and co-workers.^{24,25}

In order to investigate and study the presence of HA coating on the forsterite scaffolds, X-ray map was utilized. Figure 5 shows the X-ray map in the centre of the

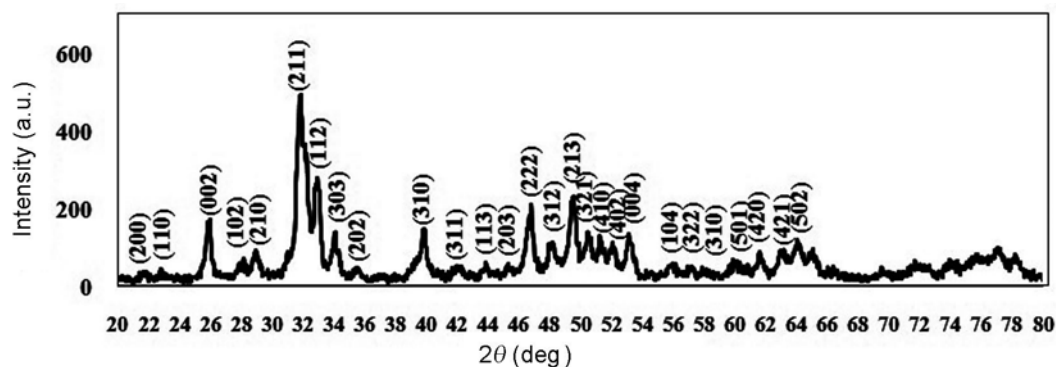


Figure 4. XRD pattern of hydroxyapatite coating.

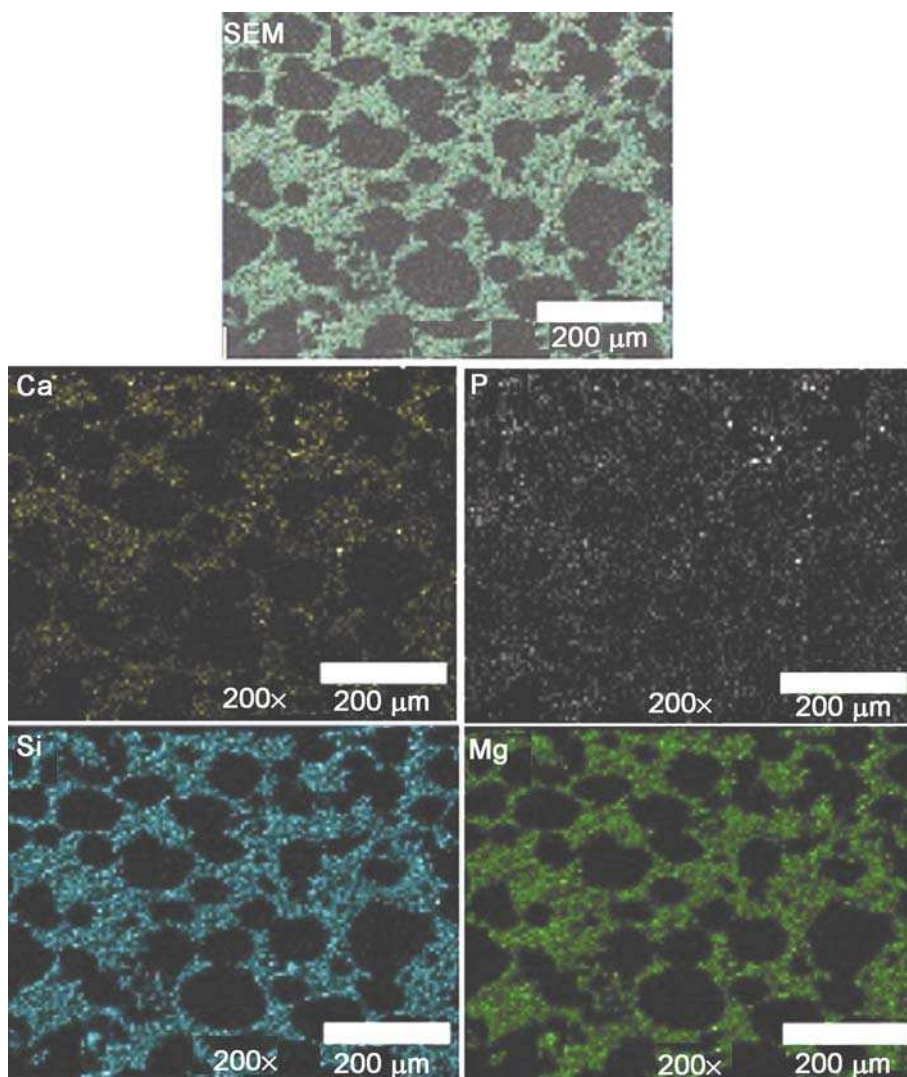


Figure 5. X-ray map of the cross-sectional surface of the hydroxyapatite-coated forsterite scaffold.

cross-cutting of HA-coated forsterite scaffold. According to figure 5, Ca and P, the main elements of HA, uniformly presented throughout the samples. Demonstrating HA coating could be formed not only on the surface porosities, but also deeply penetrated the samples.

The typical cross-section of the HA-coated forsterite scaffold is shown in figure 6c. As shown in figure 6c, elemental analysis of the inner wall of pore exhibited the presence of calcium and phosphorus, which are the main elements of HA. The thickness of the coating layer was approximately 4 μm .

The morphology and structure of as-fabricated HA-coated forsterite scaffold are shown in figure 6. As can be seen from figure 6, scaffolds had an open, interconnected and uniform porous structure with pore sizes around 65–245 μm , satisfying the requirements to allow ingrowth of osteoblast cells inside the scaffolds.³¹ Total and open porosity of these scaffolds were in the range of 75–80 and 65–70%, respectively, which were higher than

appropriate pores for bone tissue engineering and were in the ranges of the pores in cancellous bone (50–90%).³²

A typical compressive stress–strain curve of the HA-coated forsterite scaffolds is shown in figure 7. The scaffolds failed in a manner similar to the brittle bioceramic scaffolds. The elastic modulus and compressive strength of the prepared scaffolds were 291 ± 10 and 7.5 ± 0.2 MPa, respectively, which were in the range of compressive strength and elastic modulus of the cancellous bone.^{4,6,33} Enhanced compressive strength of the HA-coated forsterite scaffold compared to the results of other researchers related to the HA-coated scaffolds^{12,34,35} might be due to the nanostructured forsterite scaffold as substrate. Additionally, compared to Ghomi *et al*⁴, research compressive strength of prepared scaffold was increased. There were two reasons for the increase in compressive strength. One was the use of two-step sintering method for preparing nanocrystalline forsterite scaffold, and another was the use of HA coating. Using two-step sintering, forsterite

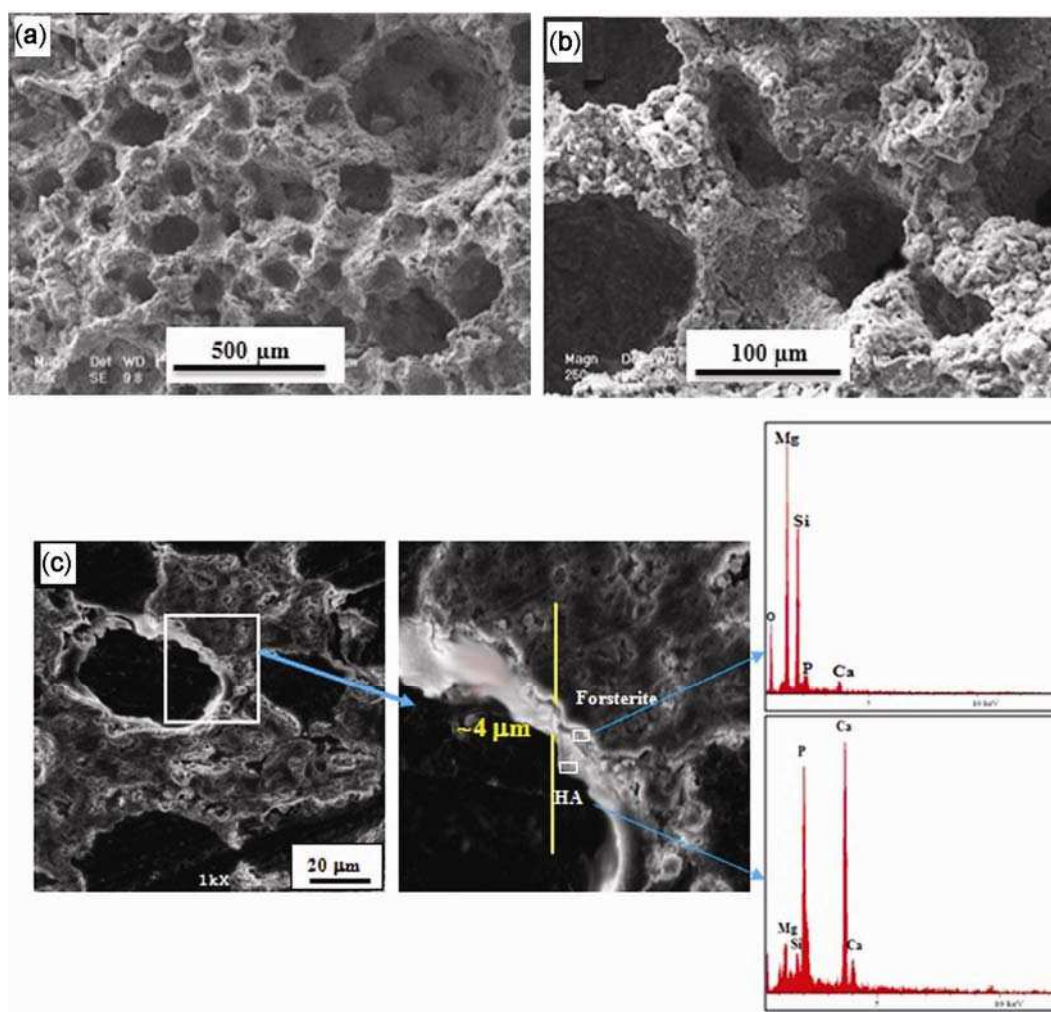


Figure 6. SEM micrographs and EDS pattern of hydroxyapatite-coated forsterite scaffold: (a, b) pore structure and (c) cross-section.

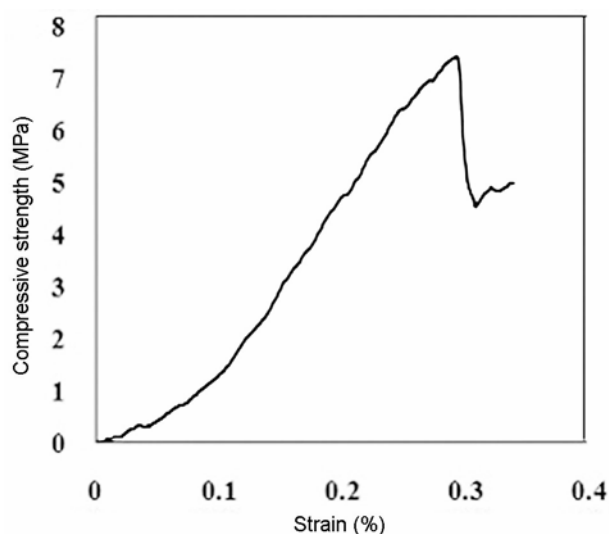


Figure 7. Compressive stress–strain curve of hydroxyapatite-coated forsterite scaffold.

scaffold with compressive strength of about 7 MPa and total porosity of about 80% was produced. By coating forsterite scaffolds with HA, HA-coated forsterite scaffold with compressive strength of about 7.5 MPa and total porosity of about 77% was produced. Mechanical properties of ceramics are strongly influenced by morphology, porosity and grain size.^{36,37} Although mechanical property of HA is lower than forsterite,¹³ the reason for this increase would be reduction in percentage and size of the porosities. It is well known that a compromise between porosity and mechanical properties exists, where an increase in the void volume and porosity results in a reduction in mechanical strength and stiffness of the scaffold.^{37,38}

Figure 8 shows the SEM micrographs of HA-coated forsterite scaffold after soaking in SBF for various periods. The agglomerated bone-like apatite particles could be observed on the surface and inner wall of the pores after 7 days of soaking. By increasing the immersion time, the number and size of these agglomerated

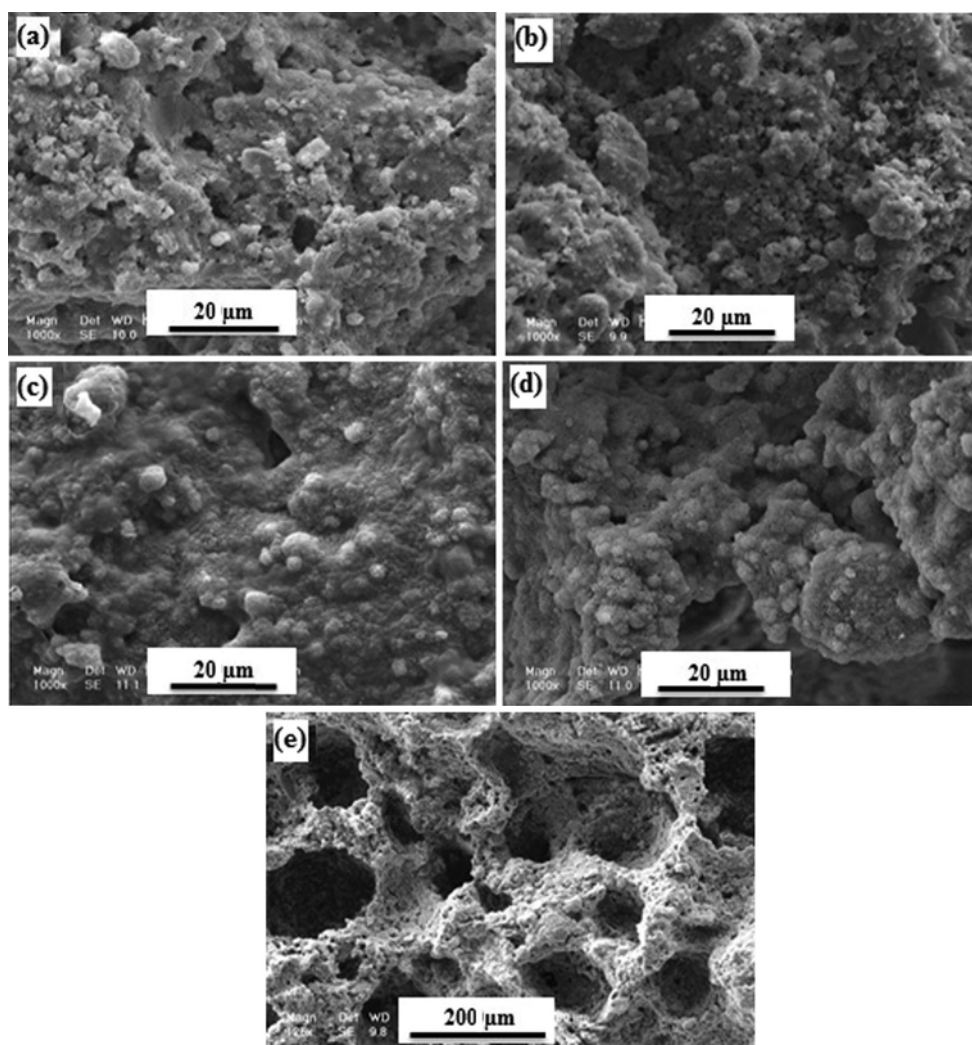


Figure 8. SEM micrographs of hydroxyapatite-coated forsterite scaffold after (a) 7, (b) 14, (c) 21 and (d, e) 28 days of immersion in SBF.

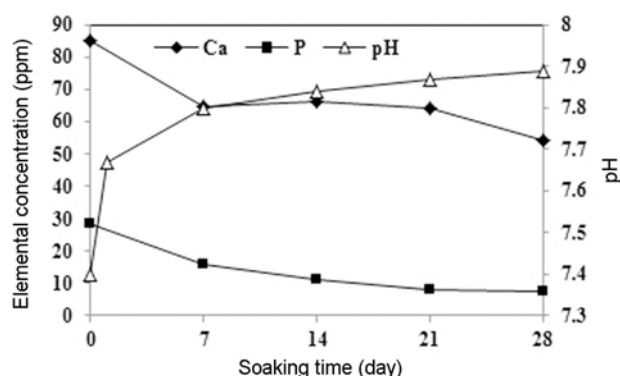


Figure 9. Changes of Ca and P concentrations and pH of the SBF solution after soaking the hydroxyapatite-coated forsterite scaffold for various periods.

particles enhanced, which resulted in a smooth surface at longer immersion time. On the other hand, bone-like apatite formation on the surface changed the morphology and size of the pores of the HA-coated forsterite scaffold.

The graph of pH changing trend in terms of soaking time is shown in figure 9. It can be seen that increasing the immersion time enhanced the pH value of SBF from 7.4 to 7.9. When HA-coated forsterite scaffold was immersed in SBF, both HA coating dissolution and deposition of bone-like apatite from the solution were occurred. At the initial stage, the dissolution rate was even slightly higher than the deposition one, resulting in an increase in pH value in near the surface regions. By increasing the immersion time, the solution near the coating surfaces was supersaturated, and the deposition rate of HA was enhanced. Therefore, after the initial stage, the HA coating was keep growing.

Figure 9 also shows the changes in the Ca and P ion concentration of the SBF after soaking the samples in SBF for various time periods. Reduction in Ca and P ion concentrations in SBF was the result of immersion of the samples in SBF.

The use of porous scaffolds for bone regeneration is one of the most common approaches in tissue engineering. Much research has been done on making HA scaffold with desired properties. The scaffolds have already had low mechanical properties.^{17,34,35} Since it is very important to increase the mechanical properties of the porous bioceramics, in the present research, the forsterite scaffold, which has better mechanical properties, was used and was coated with HA. In this case, the mechanical properties of the forsterite and the biocompatibility and bioactivity of the HA can be used simultaneously. Further studies will be focused on cell culture and *in vivo* tests on the prepared scaffolds.

4. Conclusion

Nanostructured forsterite scaffold, with crystallite size of 35–60 nm, was fabricated via the gelcasting method, and

was coated with HA by the sol–gel method in low pressure. The crystallite size of the coating was in the range of 25–29 nm. The prepared scaffold had nearly uniform, spherical and interconnected pores, with sizes in the range of 65–245 μm and with total and open porosities of about 75–80 and 65–70%, respectively. The compressive strength and elastic modulus of the prepared scaffold were 7.5 ± 0.2 and 291 ± 10 MPa, respectively, which were in the range of the compressive strength and elastic modulus of cancellous bone. The results of immersion samples in SBF proved the good bioactivity of HA-coated nanostructured forsterite scaffold in such a way that at long immersion time, bone-like apatite covered all the surface and inner wall of the scaffold pores. It seems that the collection of good mechanical properties of forsterite and favourable biological properties of HA make the HA-coated forsterite scaffold an appropriate candidate for tissue engineering and load-bearing applications.

Acknowledgement

We are grateful to Isfahan University of Technology, in particular, the Department of Materials Engineering for supporting this research.

References

1. Wu C, Chang J, Zhai W, Ni S and Wang J 2006 *J. Biomed. Mater. Res.* **78** 47
2. Ni S, Chou L and Chang J 2007 *Ceram. Int.* **33** 83
3. Kharaziha M and Fathi M H 2010 *J. Mech. Behav. Biomed. Mater.* **3** 530
4. Ghomi H, Jaberzadeh M and Fathi M H 2011 *J. Alloys Compd.* **509** 63
5. Arafa M T, Lam C X F, Ekaputra A K, Wong S Y, Li X and Gibson I 2011 *Acta Biomater.* **7** 809
6. Xu H K, Quin J B, Takagi S and Chow L C 2004 *Biomaterials* **25** 1029
7. Saki M, Narbat M K, Samadikuchaksaraei A, Ghafouri H B and Gorjipour F 2009 *Yakhteh Med. J.* **11** 55
8. Wang H, Li Y, Zuo Y, Li J, Ma S and Cheng L 2007 *Biomaterials* **28** 3338
9. Tripathi G and Basu B 2012 *Ceram. Int.* **38** 341
10. Kharaziha M and Fathi M H 2009 *Ceram. Int.* **35** 2449
11. Tavangarian F and Emadi R 2011 *Mater. Lett.* **65** 740
12. Kim H W, Knowles J C and Kim H E 2004 *Biomaterials* **25** 1279
13. Sebdani M M and Fathi M H 2011 *Int. J. Appl. Ceram. Technol.* **8** 553
14. Kosanovic C, Stubicar N, Tomasic N, Bermanec V and Stubicard M 2005 *J. Alloys Compd.* **389** 306
15. Sasikala T S, Sumab M N, Mohananb P, Pavithran C and Sebastian M T 2008 *J. Alloys Compd.* **461** 555
16. Barzegar Bafrooei H, Ebadzadeh T and Majidian H 2014 *Ceram. Int.* **40** 2869
17. Emadi R, Tavangarian F, Roohani Esfahani S I, Sheikhhosseini A and Kharaziha M 2010 *J. Am. Ceram. Soc.* **93** 2679

18. Diba M, Fathi M H and Kharaziha M 2011 *Mater. Lett.* **65** 1931
19. Diba M, Kharaziha M, Fathi M H, Gholipourmalekabadi M and Samadikuchaksaraei A 2012 *Compos. Sci. Technol.* **72** 716
20. Fathi M H and Kharaziha M 2008 *Int. J. Mod. Phys. B* **22** 3082
21. Sanosh K P, Balakrishnan A, Francis L and Kima T N 2010 *J. Alloys Compd.* **495** 113
22. Tavangarian F and Emadi R 2011 *Ceram. Int.* **37** 2275
23. Zhang F Z, Kato T, Fuji M and Takahashi M 2006 *J. Eur. Ceram. Soc.* **26** 667
24. Fathi M H and Hanifi A 2007 *Mater. Lett.* **61** 3978
25. Fathi M H, Hanifi A and Mortazavi V 2008 *J. Mater. Process. Technol.* **202** 536
26. Fathi M H and Hanifi A 2009 *Adv. Appl. Ceram.* **108** 363
27. Cullity B D 1978 *Elements of X-ray diffraction* (Windsor Locks, CT, USA: Addison-Wesley)
28. Ji S and Wang Z 1999 *Geodynamics* **28** 147
29. Erol M M, Mourino V, Newby P, Chatzistavrou X, Roether J A, Hupa L and Boccaccini A R 2012 *Acta Biomater.* **8** 792
30. Bohner M and Lemaître J 2009 *Biomaterials* **30** 2175
31. Bellucci D, Cannillo V and Sola A 2011 *Ceram. Int.* **37** 145
32. Fu Q, Saiz E, Rahaman M N and Tomsia A P 2011 *Mater. Sci. Eng.* **31** 1245
33. Dash S R, Sarkar R and Bhattacharyya S 2015 *Ceram. Int.* **41** 3775
34. Zhao J, Duan K, Zhang J W, Lu X and Weng J 2010 *Appl. Surf. Sci.* **256** 4586
35. Roohani Esfahani S I, NouriKhorasani S, Lu Z, Appleyard R and Zreiqat H 2010 *Biomaterials* **31** 5498
36. Padmanabhann S K, Gervaso F, Carrozzo M, Scalera F, Sannino A and Licciulli A 2013 *Ceram. Int.* **39** 619
37. Kusmanto F, Walker G, Gan Q, Walsh P, Buchanan F, Dickson G, McCaigue M, Maggs C and Dring M 2008 *Chem. Eng. J.* **139** 398
38. Oliveira J M, Silva S, Malafaya P B, Rodrigues M T, Kotobuki N, Hirose M, Gomes M E, Mano J F, Ohgushi H and Reis R L 2009 *J. Biomed. Mater. Res. A* **91** 175